Level scheme study of ^{91}Mo: weak-coupling approximation around $N = 50$ region

Z. Huang,[1,2] G. X. Zhang,[2,3,*] C. X. Yuan,[4] G. L. Zhang,[1,†] D. Mengoni,[2,3] B. S. Cai,[4] S. P. Hu,[5] H. Q. Zhang,[6] H. B. Sun,[7] J. J. Valiente-Dobón,[8] D. Testov,[2,3] A. Goasduff,[8] D. Bazzacco,[2,3] D. R. Napoli,[8] F. Galtarossa,[8] F. Recchia,[8] G. de. Angelis,[8] M. Siciliano,[8,9] R. Menegazzo,[8] and S. M. Lenzi[2,3]

[1]*School of Physics, Beihang University, Beijing 100191, China*
[2]*Dipartimento di fisica Astronomia dell'Universita di padova, Padova, Italy*
[3]*Istituto Nazionale di Fisica Nucleare, Sezione di Padova, Padova, Italy*
[4]*Sino-French Institute of Nuclear Engineering and Technology, Sun Yat-sen University, Zhuhai 519082, Guangdong, China*
[5]*Institute for Advanced Study in Nuclear Energy, Shenzhen University, Shenzhen 518060, China*
[6]*China Institute of Atomic Energy, Beijing 102413, China*
[7]*College of Physics and Energy, Shenzhen University, Shenzhen 518060, China*
[8]*INFN, Laboratori Nazionali di Legnaro, I-35020 Legnaro, Italy*
[9]*Physics Division, Argonne National Laboratory, Lemont-IL, USA*

(Dated: November 16, 2022)

The level scheme of ^{91}Mo has been studied using GALILEO γ-ray spectrometer at Laboratori Nazionali di Legnaro, INFN. Seven transitions together with four levels are identified for the first time by the γ-γ coincidence measurement, considerably enriching the negative band in ^{91}Mo. The discrepancy in the previous parity assignments for the states higher than 3808 keV has been clarified with the help of new experimental results. A shell-model calculation employing *JUN45* interaction is performed in order to get a further understanding of the level structure of ^{91}Mo. Being close to $N = 50$ shell closure, the weak-coupling approximation between the valence $g_{9/2}$ neutron-hole with the even-even core (^{92}Mo) is discussed in ^{91}Mo.

I. INTRODUCTION

The weak-coupling approximation, in which the discussion starts 60 years ago [1], has recently attracted a lot of attention for the study of nuclei in the semi-magic region [2–5]. Special attention is given to the early emergence of collectivity, *i.e.*, larger B(E2) values, when adding only one valence particle (or hole) to the even-even core, such as the cases of ^{129}Sb and ^{128}Sn in Ref. [2], and $N = 125$ isotones compared with the $N = 126$ ones around the ^{208}Pb region [4].

^{91}Mo (Z=42, N=49), with only one valence neutron hole in $g_{9/2}$ orbit with respect to the even-even core ^{92}Mo (Z=42, N=50), serves as a good candidate for the study of weak-coupling approximation around the ^{100}Sn region. The low-lying states in the semi-magic nucleus ^{92}Mo below ∼6 MeV are known to be pure proton configuration [6]. Therefore, the low-lying level structure of ^{91}Mo is expected to be very sensitive to the coupling or interaction between the neutron hole and the proton configurations (dominated by $\pi g_{9/2}^2$ or $\pi g_{9/2} \otimes p_{1/2}$ for positive and negative bands, respectively) as mentioned in Ref. [7].

The investigation of the ^{91}Mo began with the ^{92}Mo(d,t) reaction [8], in which the ground state was assigned as $9/2^+$ unsurprisingly. The level scheme was later extended up to 5.2 MeV in excitation energy using the ^{90}Zr(α,3nγ) reaction, identifying the positive states with spins of $13/2_1^+$, $17/2_1^+$, $21/2_1^+$, $23/2_1^+$, and $25/2_1^+$. The level structure from $9/2_1^+$ to $21/2_1^+$ shares similar energy spacings with those in yrast positive band in ^{92}Mo, indicating a possible weak-coupling between the neutron-hole and proton configurations [7].

Even though the level scheme of ^{91}Mo was significantly enriched by the following fusion-evaporation experimental works [9, 10] up to a spin of $J \sim 39/2\hbar$ with excitation energy ∼ 10 MeV, the information of negative states is quite scarce before the current work. The aforementioned Ref. [7] observed the yrast negative-parity states with spins $(17/2_1^-)$, $(25/2^1)$, $(27/2_1^-)$, $(29/2_1^-)$, and $(31/2_1^-)$. However, in Ref. [10], a polarization measurement was performed with the Clover detector, and the results tentatively alternate the parity of $(25/2_1^-)$ level at 3808-keV, giving rise to a $(25/2_2^+)$ assignment. Subsequently all the band members on top of the new $(25/2_2^+)$ level becomes $(27/2_1^+)$, $(29/2_1^+)$, and $(31/2_1^+)$. Therefore, except for the $(17/2_1^-)$ state, no negative state is known in ^{91}Mo up to now, and it is even more confusing that such a $(17/2_1^-)$ state was not observed at all in the polarization measurement [10]. More experimental efforts are necessary in order to get further information on the level scheme of ^{91}Mo, especially for the negative-parity states which are well established in the neighboring nuclei, *i.e.*, ^{92}Mo (see Fig. 1 in Ref. [11]) and ^{93}Ru (see Fig. 7 in Ref. [12]).

The paper is organized as follows. The experimental setup is shown in Sec. II. Sec. III presents the data analysis and results. The shell model calculation are discussed in Sec. IV and a summary of the work will be finally given in Sec. V.

* E-mail address: guangxin.zhang@pd.infn.it
† E-mail address: zgl@buaa.edu.cn

II. EXPERIMENTAL SETUP

In order to study the level structure of ^{91}Mo, a ^{6}Li+^{89}Y experiment was performed at INFN-LNL, Italy. The ^{6}Li beam was accelerated up to 34 MeV by Tandem-XTU accelerator and impinging on a ^{89}Y target of 550 μg/cm^2 thickness. The average beam intensity was 1.0 enA. A ^{12}C foil with a thickness of 340 μg/cm^2 was backed on the ^{89}Y target in order to stop all the fusion-evaporation residues, including ^{91}Mo. The γ rays emitted from the residues were collected by the high-resolution detector array called GALILEO [13], consisting of 25 Compton-suppressed high-purity germanium (HPGe) tapered detectors during the current Phase-I configuration. Each HPGe detector is surrounded by eight BGO crystals as the anti-Compton shield. All the HPGe detectors were arranged into four rings with different angles with respect to the beam direction: ten detectors were placed at 90°, and other fifteen detectors were mounted equally at 119° (5 detectors), 129° (5 detectors) and 152° (5 detectors), respectively. Each detector was put 235 mm away from the target position. The typical energy resolution of GALILEO array was measured to be 0.17% at 1.3 MeV. The efficiency for each detector was calibrated by ^{60}Co, ^{133}Ba, ^{152}Eu, ^{88}Y, and ^{241}Am sources with known radioactivity placed at the target position. The typical efficiency for the whole array was 2.5 % at 1 MeV.

The data acquisition system of the GALILEO array was fully digitalized based on the XDAQ framework [14, 15]. Different digitizers were synchronized by a distributed clock using Global Trigger System (GTS) with a frequency of 100 MHz, giving a common absolute time (timestamp) for each γ ray. In the following analysis, γ rays measured by different HPGe detectors were merged into a same event when their absolute time difference was smaller than 500 ns, allowing for a prompt or delayed γ-γ coincidence analysis which would be discussed in details later. The detailed information on the experimental setup can be found in the previous publications [13, 16].

III. DATA ANALYSIS AND RESULTS

The partial level scheme of ^{91}Mo constructed in the current work is shown in Fig. 1. In addition to the previous studies in Refs. [7, 9, 10, 17], seven transitions together with four levels are identified for the first time, marked with the color red in Fig. 1. All these new transitions can be clearly observed in the coincidence spectra gated by the 1414 keV γ ray ($13/2^+_1 \rightarrow 9/2^+_{g.s.}$) in ^{91}Mo, as shown in Fig. 2 (a) and Fig. 3 (a) with different energy regions.

The newly observed transitions at 409-, 497-, 609-, 623-, and 1032-keV are placed on top of the long-lived isomer at 2279 keV with J^π=($17/2^-_1$). The half-life of this isomer was measured to be 38(4) ns via α-γ time difference method in a ^{90}Zr(α, 3nγ) experiment [7]. In the current work, an delayed coincidence γ-ray spectrum collected in a time window of 60 - 500 ns earlier than the 211-keV transition (depopulating the isomer) is shown in Fig. 2 (b). The aforementioned transitions at 409-, 497-, 609-, 623-, and 1032-keV are clearly seen in the delayed coincidence spectrum, being the main argument of the current assignment. The detailed position of each transition can be fixed by the further $\gamma-\gamma$ coincidence analysis as well as their energy and intensity relationships as listed in Table I. It should be mentioned here that the relative intensities of only strong transitions at 1414-, 654-, 211- and 199-keV are directly derived from the single γ-ray spectrum. All the other weak transitions, including the newly observed ones, are obtained by the 1414-keV gated spectrum.

Because of the low statistics for most of the newly observed transitions in this work, only 409- , 623- and 1032-keV γ rays can be analyzed in terms of γ-ray angular distribution ratio from oriented nuclei (*ADO* ratio) [18]. The *ADO* ratio of γ ray in the present setup is defined as:

$$R_{ADO} = \frac{I_{\gamma_1} \text{at } 152^\circ, \text{ gated with } \gamma_2 \text{ at any angle}}{I_{\gamma_1} \text{at } 90^\circ, \text{ gated with} \gamma_2 \text{ at any angle}},$$

here γ_1 and γ_2 are assumed to be cascading transitions in one oriented nucleus, and I_γ represents the intensity of transition after efficiency corrections. By comparing with the R$_{ADO}$ values of γ-rays whose multipolarities are well known in ^{91,92}Mo, ^{92}Nb, ^{89}Zr produced in the same work as shown in Fig. 4, the 409- and 623-keV transitions are determined to be dipole γ rays, while the 1032-keV transition is a quadrupole nature. Therefore, the spin-parities of newly established levels at 2902- and 3311-keV are assigned to be ($19/2^-_1$) and ($21/2^-_1$), by assuming a $M1$ characters for 409- and 623-keV γ rays, and $E2$ character for the 1032 keV one. It should be noticed here that the assignments of spin-parity for the newly observed states are still tentative due to the lack of polarization measurement in the current work. Nevertheless, very similar structure on top of the negative-parity isomer can be found in the neighbouring odd-even ^{93}Ru, see Fig. 7 in Ref. [12]. The underlying physics, especially the coupling between valence neutron-hole and even-even core, will be discussed in the following section.

The current work also modifies the parities of the states at 2218- and 2293-keV according to the new experimental results. Since the R$_{ADO}$ ratio of 879-keV transition, which connects 2293- and 1414-keV ($13/2^+_1$) levels, is measured to be 1.32(32) in this work. Such value stands between the limitations of stretched dipole and quadrupole transitions, being most likely a mixed M1/E2 nature. As a result, the parity of the 2293-keV state is modified to positive, giving rise to a ($15/2^+_1$) level. On the other side, the R$_{ADO}$ ratio of the 804-keV transition is well consistent with the stretched dipole nature as shown in Fig. 4, giving rise to a $E1$ assumption. Therefore, the J^π of initial state at 2218 keV is modified from

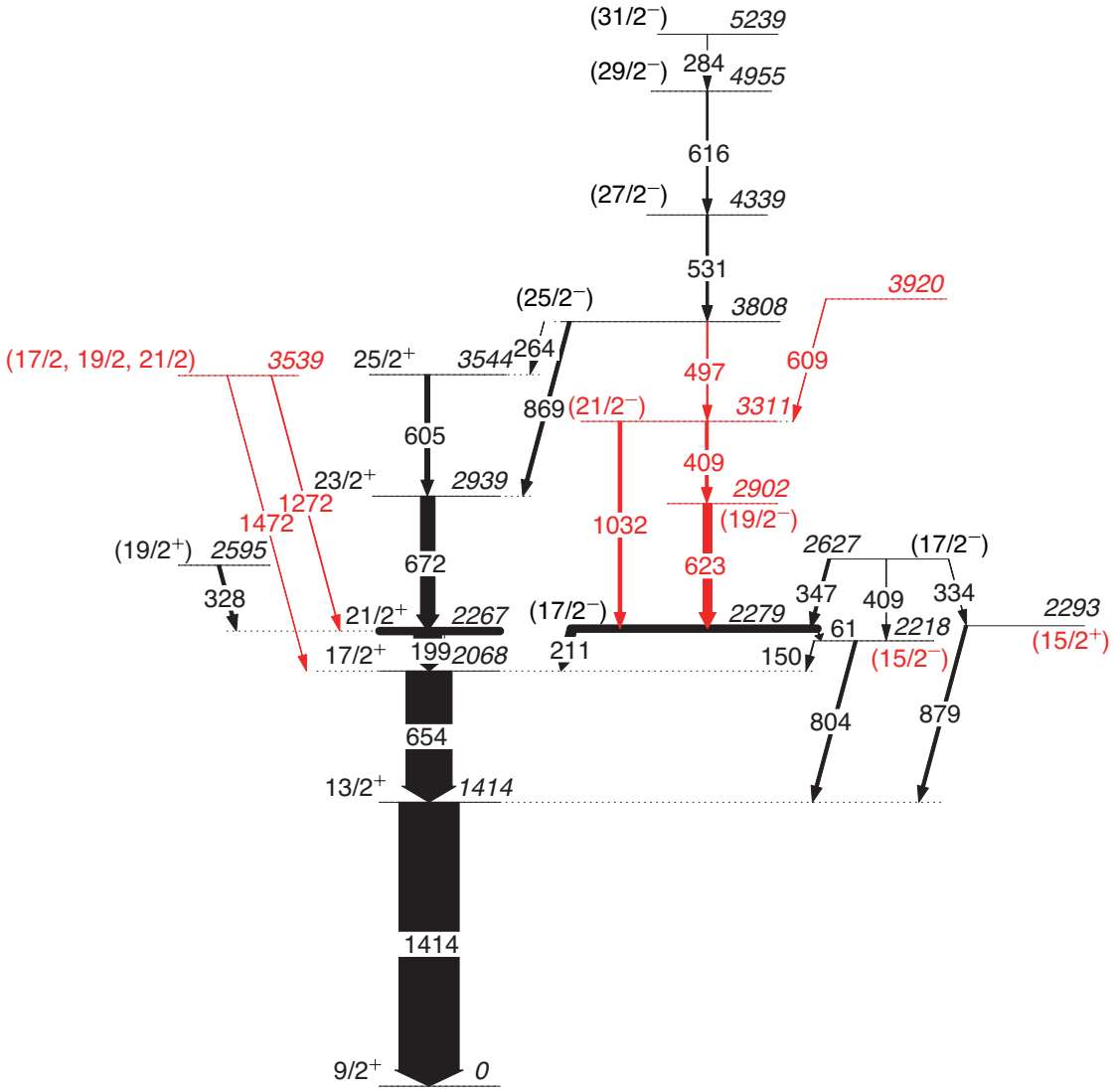

FIG. 1. (Color online)Level scheme of ^{91}Mo. The levels measured in the current work are shown in red color. The width of the arrows indicates γ-ray intensities, while the energies are given in keV units.

$(15/2^+_1)$ to $(15/2^-_1)$. The current assignment can be well reproduced by shell model calculation, which would be discussed later in next section.

A new state at 3539-keV was identified in ^{91}Mo by comparing Figures 3 (a) and (b), the coincidence spectra with gates on 1414- and 199-keV (delayed coincidence due to the existence of the isomer at 2267 keV) transitions, respectively. The results show that both of them see 1272-keV line clearly, while 1472-keV peak only exists in the former one. Considering the energies of these three γ rays, a cascading 199-1272-keV transitions are put in parallel with 1472-keV γ ray, giving rise to a new state at 3539-keV as shown in Fig. 1. The R_{ADO} ratio information for the 1272- and 1472-keV transitions is not available, therefore the spin for the 3539-keV level might be 17/2, 19/2 or 21/2 due to the fact that it can decay towards the $21/2^+_1$ and $17/2^+_1$ states simultaneously.

Since the 623- and 1032-keV γ rays, which directly feed the $J^\pi=(17/2^-_1)$ isomer, are observed for the first time, the lifetimes of the $(17/2^-_1)$ isomer in ^{91}Mo can be re-measured with the γ-γ time-difference method. Figures 5 (a) and (b) show the time difference spectra between transitions directly feeding and de-exciting the $21/2^+_1$ and $(17/2^-_1)$ states, respectively. The deconvolution fitting [19] gives a half-life of 47(4) ns for the $(17/2^-_1)$ state, which is higher than 38(4) ns obtained from the aforementioned $\alpha-\gamma$ time-difference measurement [7]. On the other hand, half-life of the $21/2^+_1$ is measured to be 49(1) ns in this work, being not only higher but also more precise than the previous result of 40(4) ns from Ref. [7].

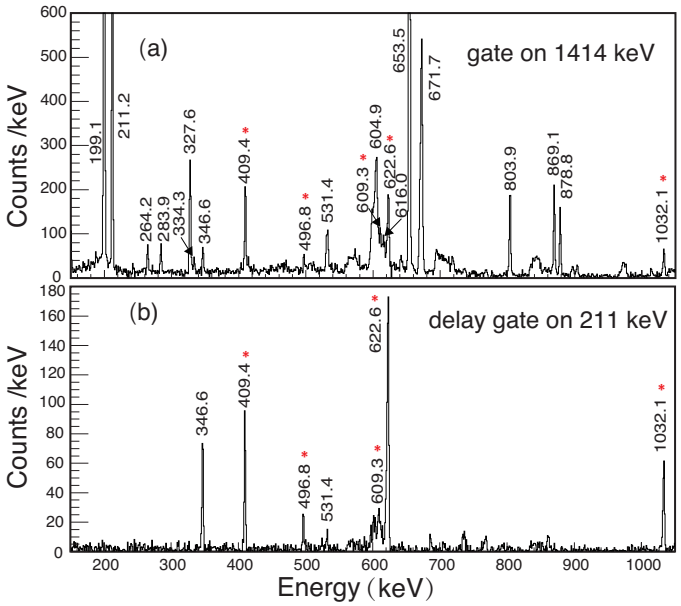

FIG. 2. Gamma-ray coincidence spectra with (a) a gate (time window: ±500 ns) on 1414 keV γ-ray, (b) a delayed coincidence gate (time window: -500,-60 ns) on 211 keV γ-ray. All the new transitions are labeled with asterisk(*).

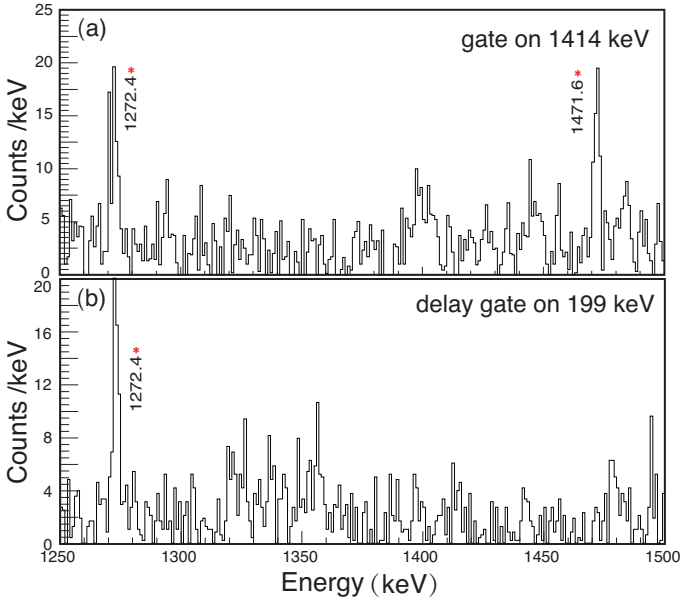

FIG. 3. Gamma-ray coincidence spectra with (a) a gate (time window: ±500 ns) on 1414 keV γ-ray, (b) a delay gate (time window: -500,-60 ns) on 199 keV γ-ray. All the new transitions are labeled with asterisk(*).

IV. SHELL MODEL CALCULATION AND DISCUSSION

In order to get a further understanding of the experimental level structure in ^{91}Mo, a shell-model calculation using JUN45 interaction[21] was performed using the KSHELL code [20]. Both proton and neutron valence spaces include the $p_{3/2}$, $f_{5/2}$, $p_{1/2}$, and $g_{9/2}$ orbits with the ^{56}Ni as the inert core. The interaction is firstly obtained with a realistic one based on the Bonn-C potential and then modified empirically in order to reproduce around 400 experimental levels of 69 nuclei with mass numbers A=63∼96. The JUN45 calculated results are compared with the selected experimental levels as shown in Fig. 6. Table II summarizes the main configurations for each predicted level. It can be seen that the shell-model calculation reasonably reproduces the experimental levels in ^{91}Mo, and the deviation even gets smaller for the higher-spin states. For the new levels as well as the states with new spin-parity assignments, including the $(15/2^+_1)$, $(15/2^-_1)$, $(19/2^-_1)$ and $(21/2^-_1)$ levels (marked red in Fig. 6), the shell-model calculation succeeds not only in predicting their position, but also in their ordering with respect to the neighboring states.

In this section, the discussion firstly focus on the spin-parity assignment for the 3808-keV state. Later on a

TABLE I. Gamma transition energy (E_γ) in keV, relative intensity(I_γ), γ-ray angular distribution from oriented nuclei(ADO) ratios, spin-parities for the initial and final states of observed transitions in ^{91}Mo. The quoted errors on intensity and R_{ADO} encompass errors due to the background-subtraction, fitting and efficiency correction. The new transitions are indicated with an asterisk(*), the blank indicates no relative information in the current work.

E_γ (keV)	I_γ (relative)	R_{ADO}	$J_i^\pi \rightarrow J_f^\pi$
61.0(3)	1.3(2)[a]		$(17/2^-) \rightarrow (15/2^-)$
149.6(1)	2.0(5)[a]		$(15/2^-) \rightarrow 17/2^+$
199.1(1)	55.3(17)	1.56(9)	$21/2^+ \rightarrow 17/2^+$
211.2(2)	13.1(4)	1.66(17)	$(17/2^-) \rightarrow 17/2^+$
264.2(1)	1.2(2)[a]		$(25/2^-) \rightarrow 25/2^+$
283.9(1)	1.5(2)[a]		$(31/2^-) \rightarrow (29/2^-)$
327.6(1)	6.8(5)[a]	1.03(12)	$(19/2^+) \rightarrow 21/2^+$
334.3(1)	0.7(1)[a]		$(17/2^-) \rightarrow (15/2^+)$
346.6(1)*	1.6(2)[a]	1.58(28)	$(17/2^-) \rightarrow (17/2^-)$
409.4(1)[b]	≤4.6(4)[a]		$(17/2^-) \rightarrow (15/2^-)$
409.4(1)*[b]	≤4.6(4)[a]	0.81(11)	$(21/2^-) \rightarrow (19/2^-)$
496.8(1)*	1.1(2)[a]		$(25/2^-) \rightarrow (21/2^-)$
531.4(1)	4.1(4)[a]	1.08(16)	$(27/2^-) \rightarrow (25/2^-)$
604.9(1)	7.9(8)[a]		$25/2^+ \rightarrow 23/2^+$
609.3(1)			
616.0(1)			$(29/2^-) \rightarrow (27/2^-)$
622.6(1)*	8.1(6)[a]	0.82(16)	$(19/2^-) \rightarrow (17/2^-)$
653.5(1)[b]	≤76.3(23)	1.62(9)	$17/2^+ \rightarrow 13/2^+$
671.7(1)	28.2(17)[a]	1.07(13)	$23/2^+ \rightarrow 21/2^+$
803.9(1)	7.3(5)[a]	0.99(21)	$(15/2^-) \rightarrow 13/2^+$
869.1(1)	7.2(6)[a]	1.17(17)	$(25/2^-) \rightarrow 23/2^+$
878.8(1)	5.7(5)[a]	1.32(32)	$(15/2^+) \rightarrow 13/2^+$
1032.1(1)*	3.1(3)[a]	1.80(39)	$(21/2^-) \rightarrow (17/2^-)$
1272.4(1)*	1.2(2)[a]		$(17/2,19/2,21/2) \rightarrow 21/2^+$
1414.1(1)	100(3)	1.68(11)	$13/2^+ \rightarrow 9/2^+$
1471.6(1)*	1.2(2)[a]		$(17/2,19/2,21/2) \rightarrow 17/2^+$

(a) Estimated from coincident data gating on 1414.1-keV γ ray.
(b) Doublets in ^{91}Mo.

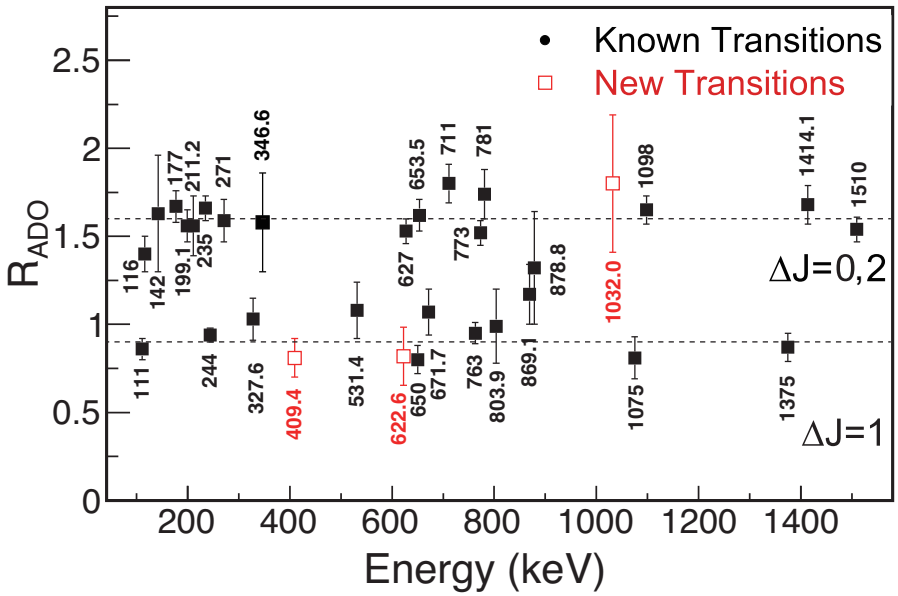

FIG. 4. R_{ADO} plotted for γ-ray transitions of ^{91}Mo. The lines correspond to the value of R_{ADO} for the known quadrupoles and dipoles. The quoted error includes the error due to the background subtraction, fitting, and efficiency correction.

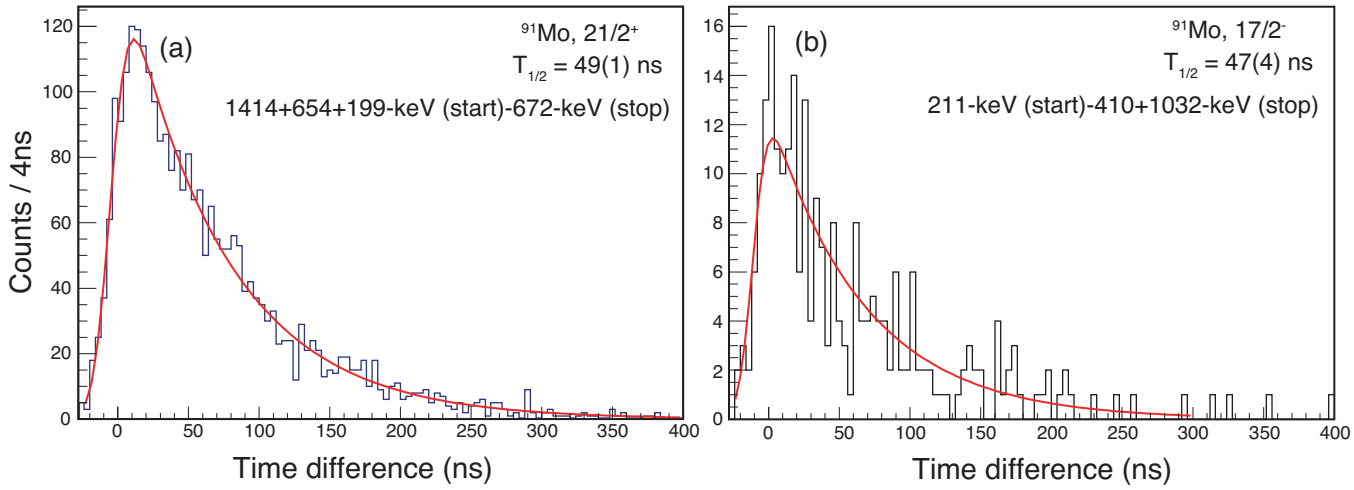

FIG. 5. The delayed time distribution spectra. Time difference of γ rays populating and depopulating (a) $21/2^+$ and (b) $17/2^-$ states.

special attention is given to the weak-coupling approximation in ^{91}Mo level structure, in terms of a coupling between a valence $g_{9/2}$ neutron hole with the core-excitation from the neighboring even-even core of ^{92}Mo.

A. The spin-parity of the 3808 keV state

As mentioned in the introduction part, the states at 3808-, 4339-, 4955-, 5239-keV were firstly found in the α+^{90}Zr fusion evaporation reaction [7]. In that work, according to the Doppler-shift analysis, the 869-keV γ ray which de-excites the 3808-keV level to the $23/2^+$ state should have a $E1$ nature (since the lifetime of the initial state is roughly estimated to be within 10^{-11}-10^{-8} s range), giving rise to a $(25/2^-_1)$ assignment for the initial state. This assignment was confirmed later by another experimental work [9], in which the half-life of the 3808 keV state was measured to be 17(3) ps, being consistent with the Doppler-shift analysis.

However, S. Ray et al. [10] tentatively assigned a J^π=$(25/2^+_2)$ to the 3808-keV state based on a possible mixed $M1/E2$ nature of the 869-keV transition by a Clover measurement. As can be seen in Fig. 4 of Ref. [10], the asymmetry parameter for the 869-keV transition, which is employed to distinguish electric and magnetic nature, stays very close to zero, and indeed the large error bar can even cross zero. However, at the same time, the 244-keV transition in the neighbouring ^{92}Mo, which was also produced in the same experiment [22], shows nearly the same asymmetry parameter (close to zero). The 244-keV transition was confirmed to be the transition between the 5^-_1 and 4^+_1 states, being a $E1/M2$ nature (see Ref. [11] for the detailed discussion). Therefore, the nearly zero value of asymmetry parameter for the 869-keV transition could also predicts a $E1/M2$ nature. If considering the measured lifetime of 3808-keV level, the $E1/M2$ assumption for the 869-keV transition would give a strong hinderance factor (larger than 10^4) for $E1$ strength which is quite common in this region, since no single-particle orbits near the Fermi surface can be connected by $E1$ operator (see Ref. [7, 11, 23] and references therein).

The J^π=$(25/2^-_1)$ assignment for the 3808-keV level is consistent with the JUN45 calculation not only on the energy side (shell-model prediction is 3776 keV, as shown in Fig. 6), but also on the decay pattern as discussed below. In the current work, a 497-keV transition is observed for the first time, connecting the 3808-keV state and the $(21/2^-_1)$ state. With the assumption of J^π=$(25/2^-_1)$ for the 3808-keV level, the 497-keV γ ray should be a pure E2 transition with B($E2$) = 5.3(10) *W.u.* obtained with the help of the previously measured half-life of the initial state [9] and the current branching ratio information. The JUN45 calculation predicts a B($E2$) value of 3.1 *W.u.* for the $25/2^-_1 \rightarrow 21/2^-_1$ transition, being well consistent with the experimental result.

However, if assuming a $(25/2^+_2)$ nature for the 3808-keV state, then the corresponding 497-keV transition would be a $M2$ character with B($M2$) around 348 *W.u.*. Such enhanced $M2$ transition is very difficult to be explained in the current Z∼40, N∼50 region. On the other hand, the JUN45 calculation predicts two $25/2^+$ levels as shown in Fig. 6. The first one matches with the experimental observed $25/2^+_1$ state at 3543-keV. If the experimental level at 3808 keV has J^π=$(25/2^+_2)$, the deviation between the experimental data and the theoretical calculation would be around 600 keV for this level, which is significantly larger than the normal discrepancies around 300 keV for the other low-lying levels in ^{91}Mo. In fact, the calculated $25/2^+_2$ state would match another previous known experimental state at 4444 keV (not found in the current work owing to the limited statistics) which mainly depopulated by a 2177 keV transition to the $21/2^+_1$ state, the details information on this 4444-keV state can be found in Fig. 5 from Ref. [9] and Fig. 5 from Ref. [10].

As a short summary, based on the aforementioned arguments, the 3808-keV state is re-assigned as J^π=$(25/2^-_1)$ in the current work, along with the $(27/2^-_1)$, $(29/2^-_1)$, and $(31/2^-_1)$ assignments to the states at 4339-, 4955-, and 5239-keV, being consistent with the previous two experimental works [7, 9]. The similar level structure systematically exists in the neighboring ^{93}Ru ($Z = 44$, $N = 49$) which can be found in Fig. 7 of Ref. [12].

B. Weak-coupling approximation

In this section, we want to investigate to what extent the low-lying states in ^{91}Mo comply with the weak coupling approximation between a valence $g_{9/2}$ neutron hole and the core-excitation of the neighboring even-even ^{92}Mo. The basic description of weak-coupling approximation and its effect on level structure of odd-A isotopes can be found in Ref. [1].

Assuming an $E2$ transition in the odd-even nucleus, in which both the initial (J_i) and final (J_f) states can be viewed as the coupling between the same valence j nucleon and different core-excited states of J_c and J'_c, the corresponding $B(E2)$ can be written as below:

$$B(E2; J_i \rightarrow J_f) = \frac{\alpha_2}{(2J_i+1)} | < J'_c\ j, J_f || \Omega^{(2)} || J_c\ j, J_i > |^2,$$

here the α_2 is a constant value and $\Omega^{(2)}$ represents the electric quadrupole operator. In the weak-coupling approximation, there is no interaction between the valence particle (hole) and the core-excitation, thus the quadrupole operator could be separated into two parts. One works only on the core and the other on the valence particle (hole), namely, $\Omega^{(2)} = \Omega^{(2)}_c + \Omega^{(2)}_p$. Therefore, the $E2$ transition matrix element can be also separated

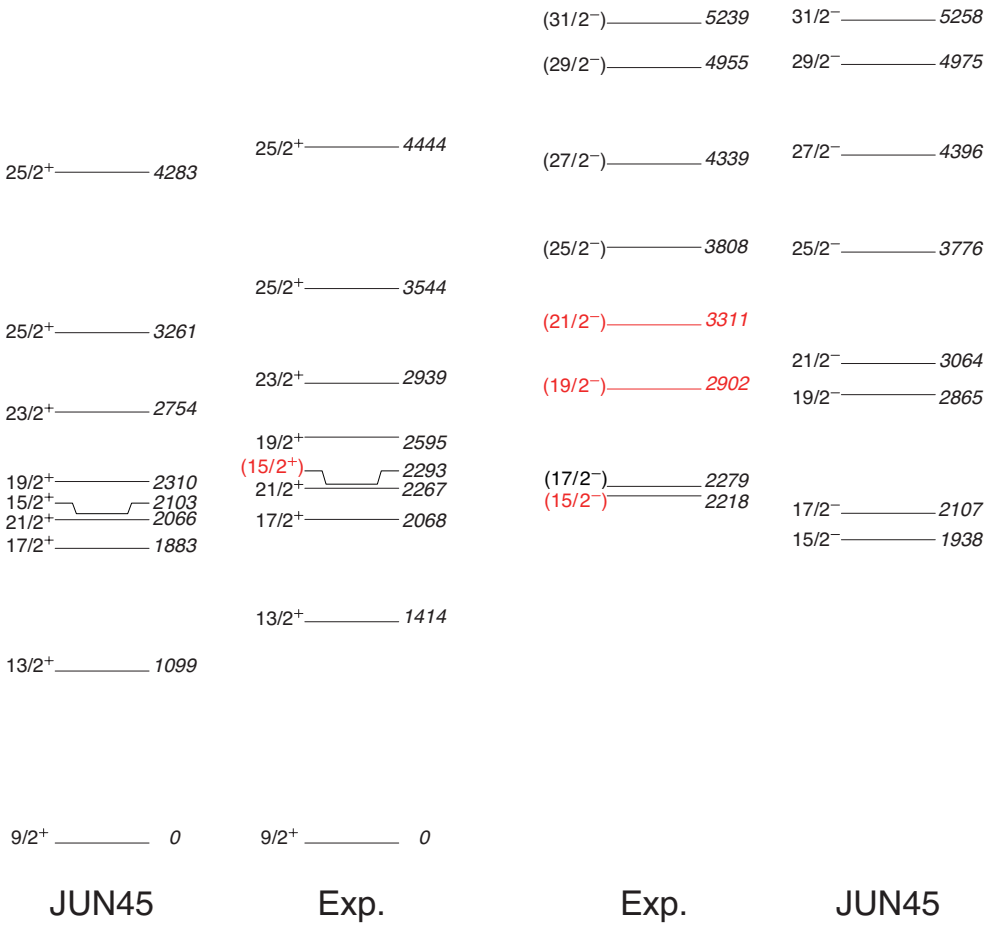

FIG. 6. Comparison between the observed excitation energies and the shell-model calculations for ^{91}Mo. The excitation energies are shown in keV unit. Experimental results suggested by the current work are shown in red color.

into two parts as listed below:

$$
\begin{aligned}
&< J'_c\ j, J_f||\Omega_c^{(2)} + \Omega_p^{(2)}||J_c\ j, J_i > \\
&= (-1)^{J'_c+j+J_f}[(2J_f+1)(2J_i+1)]^{1/2} \\
&\times [< J'_c||\Omega_c^{(2)}||J_c > \begin{Bmatrix} J'_c & J_f & j \\ J_i & J_c & 2 \end{Bmatrix} \\
&+ (-1)^{J_i-J_f} < j||\Omega_p^{(2)}||j > \begin{Bmatrix} j & J_f & J_c \\ J_i & j & 2 \end{Bmatrix} \delta_{J_c J'_c}].
\end{aligned}
$$

As mentioned before, the initial and final states correspond to different core-states, and the second term on the right-hand side vanishes accordingly. Thus the $B(E2)$ of assumed transition becomes

$$
\begin{aligned}
&B(E2; J_i \rightarrow J_f) = \\
&\alpha_2(2J_f+1)\begin{Bmatrix} J'_c & J_f & j \\ J_i & J_c & 2 \end{Bmatrix}^2 | < J'_c||\Omega_c^{(2)}||J_c > |^2.
\end{aligned}
$$

On the other side, in the even-even core the corresponding transition should has $B(E2; J_c \rightarrow J'_c) = \frac{\alpha_2}{2J_c+1}| < J'_c||\Omega_c^{(2)}||J_c > |^2$. The difference between $B(E2; J_c \rightarrow J'_c)$ in even-even core and $B(E2; J_i \rightarrow J_f)$ in odd-A nuclide only exists between coefficients before the transition elements, *i.e.*, $(2J_f+1)\begin{Bmatrix} J'_c & J_f & j \\ J_i & J_c & 2 \end{Bmatrix}^2$ and $\frac{1}{2J_c+1}$. In the special case of $J_i = J_c + j$, $J_f = J'_c + j$, and $|J_i - J_f| = 2$ (stretched $E2$ transition), the $\begin{Bmatrix} J'_c & J_f & j \\ J_i & J_c & 2 \end{Bmatrix}^2$ can be proven to be equal to $\frac{1}{(2J_c+1)(2J_f+1)}$ with the help of online 6-j symbol calculator [24], giving rise to the fact that the stretched $E2$ strengths in odd-A nucleus should be exactly the same with that in corresponding $J_c \rightarrow J'_c$ transitions in neighboring even-even core under the weak-coupling approximation.

Now we change to the comparison between the experimental levels in ^{91}Mo (see Fig. 1) and ^{92}Mo (see Fig. 1 in Ref. [6] for instance). It can be found that the excitation energies of the $9/2^+_1$, $13/2^+_1$, $17/2^+_1$, $21/2^+_1$ states in ^{91}Mo are very similar with the 0^+_1, 2^+_1, 4^+_1, 6^+_1 states in ^{92}Mo. Same situation exists for the $(17/2^-_1)$, $(21/2^-_1)$, $(25/2^-_1)$ states in ^{91}Mo and the 5^-_1, 7^-_1, 9^-_1 states in ^{92}Mo. Therefore, simply considering the level energies, the weak-coupling between a valence $g_{9/2}$ neutron hole with the core-excitation of even-even ^{92}Mo still preserves in low-lying states of ^{91}Mo, at least for the level with excitation energy lower than 3.8 MeV.

However, the $B(E2)$ value for the $21/2^+_1 \rightarrow 17/2^+_1$ transition is deduced to be 33.9(7) e^2fm^4 in ^{91}Mo from the current lifetime measurement (see Sec. III), being 2 times smaller than the corresponding $B(E2; 6^+_1 \rightarrow 4^+_1)$=81.9(14) e^2fm^4 in ^{92}Mo (measured in Ref. [6] within the same experiment). This discrepancy destroys the weak-coupling approximation between the $21/2^+_1$ state in ^{91}Mo and the 6^+_1 state in ^{92}Mo.

Now we change discussion to the higher-lying states, focusing on the $23/2^+_1$ (2939 keV) and $25/2^+_1$ (3544 keV) states in ^{91}Mo which were interpreted as members of multiplets formed by the coupling of $g_{9/2}$ neutron hole with the 8^+_1 state in ^{92}Mo in the previous work [7]. Meanwhile, the $25/2^+_1$ state decay solely via a $M1$ transition towards the $23/2^+_1$ level which belongs to the same multiplets, and there is no stretched $E2$ transition connecting the $25/2^+_1$ state and the $21/2^+_1$ state which is supposed to be the member of next mutiplets, being very different with the expectation of weak-coupling approximation.

As a result, even though the energy level scheme is quite similar between ^{91}Mo and ^{92}Mo (especially for the low-lying parts), the reduced transition probability as well as the decay pattern, which are very sensitive to the overlap between wave-functions of the initial and final states, suggest that states higher than 2.2 MeV in ^{91}Mo deviate from the weak-coupling approximation. It is even more interesting to notice that, within a simple consideration, the coupling of a neutron-hole to ^{92}Mo would induce a fragmentation of wave-function, if the interaction between the valence neutron hole to the even-even core is not negligible. Thus an enhanced collectivity should be expectation in ^{91}Mo compared with ^{92}Mo. However, as mentioned before, the experimental result shows that B($E2$) value in ^{91}Mo becomes smaller, which may indicate some de-constructive interference between different contributions after involving the strong or weak coupling effect. In order to have a further understanding of coupling effect in this nuclear region, more efforts from the experimental side, including the lifetime measurement of more comparable states in odd-even and even-even nuclei are highly demanded.

V. SUMMARY

In the current work, ^{91}Mo was produced using the ^{6}Li + ^{89}Y fusion evaporation reaction performed at LNL-INFN. The level scheme of ^{91}Mo, in particular the negative-parity part, was considerably enriched by the $\gamma-\gamma$ coincidence measurement employing the GALILEO spectrometer. The lifetimes of two isomeric states in ^{91}Mo were also remeasured using the same $\gamma-\gamma$ time-difference method with the help of newly observed transitions. Angular distribution ratios of γ rays emitted from oriented ^{91}Mo were obtained in order to get the multi-polarity information. The problem of parity assignment for the 3808-keV level was clarified based on the new experimental result. The partial level scheme of ^{91}Mo proposed in this work can be well reproduced by JUN45 calculation. In ^{91}Mo, the weak-coupling approximation between the valence neutron hole and the ^{92}Mo core seems to be fine for low-lying states if one just looks at the similarities in energy levels. However, regarding the discrepancy at the experimental B(E2), the weak-coupling approximation breaks down for states higher than 2 MeV. More lifetime information for the low-lying states in ^{91}Mo is highly desired so as to investigate the potential drop in collectivity or B(E2) values.

TABLE II. Main configurations ($\geq$ 10%) of wave functions for each level in ^{91}Mo. Each partition is form of $P = [\pi(p(1),p(2),p(3),p(4)) \otimes \nu(n(1),n(2),n(3),n(4))]$. Here, $p(i)$ represents the number of protons occupying the $p_{3/2}$, $f_{5/2}$, $p_{1/2}$, and $g_{9/2}$ orbits, and $n(i)$ represents the number of neutrons occupying the $p_{3/2}$, $f_{5/2}$, $p_{1/2}$, and $g_{9/2}$ orbits.

J ($\hbar$)	E$_x$ (keV)	Wave function	Partitions (%)
$9/2^+$	0	π(4,6,2,2)$\otimes\nu$(4,6,2,9)	42.11
		π(4,6,0,4)$\otimes\nu$(4,6,2,9)	19.34
		π(2,6,2,4)$\otimes\nu$(4,6,2,9)	13.82
$13/2^+$	1099	π(4,6,2,2)$\otimes\nu$(4,6,2,9)	54.41
		π(4,6,0,4)$\otimes\nu$(4,6,2,9)	11.25
		π(2,6,2,4)$\otimes\nu$(4,6,2,9)	9.73
$17/2^+$	1883	π(4,6,2,2)$\otimes\nu$(4,6,2,9)	55.61
		π(4,6,0,4)$\otimes\nu$(4,6,2,9)	12.29
$21/2^+$	2066	π(4,6,2,2)$\otimes\nu$(4,6,2,9)	55.64
		π(4,6,0,4)$\otimes\nu$(4,6,2,9)	12.73
$15/2^+$	2103	π(4,6,2,2)$\otimes\nu$(4,6,2,9)	56.64
		π(4,6,0,4)$\otimes\nu$(4,6,2,9)	11.27
$19/2^+$	2310	π(4,6,2,2)$\otimes\nu$(4,6,2,9)	59.57
		π(4,6,0,4)$\otimes\nu$(4,6,2,9)	11.33
$23/2^+$	2754	π(4,6,2,2)$\otimes\nu$(4,6,2,9)	54.82
		π(4,6,0,4)$\otimes\nu$(4,6,2,9)	16.19
		π(2,6,2,4)$\otimes\nu$(4,6,2,9)	10.68
$25/2_1^+$	3261	π(4,6,2,2)$\otimes\nu$(4,6,2,9)	49.91
		π(4,6,0,4)$\otimes\nu$(4,6,2,9)	20.56
		π(2,6,2,4)$\otimes\nu$(4,6,2,9)	12.42
$25/2_2^+$	4283	π(4,6,0,4)$\otimes\nu$(4,6,2,9)	57.95
		π(2,6,2,4)$\otimes\nu$(4,6,2,9)	9.85
$15/2_1^-$	1938	π(4,6,1,3)$\otimes\nu$(4,6,2,9)	61.61
		π(2,6,1,5)$\otimes\nu$(4,6,2,9)	8.17
$17/2_1^-$	2107	π(4,6,1,3)$\otimes\nu$(4,6,2,9)	69.97
		π(2,6,1,5)$\otimes\nu$(4,6,2,9)	9.57
$19/2^-$	2865	π(4,6,1,3)$\otimes\nu$(4,6,2,9)	72.73
		π(2,6,1,5)$\otimes\nu$(4,6,2,9)	11.09
$17/2_2^-$	2907	π(4,6,1,3)$\otimes\nu$(4,6,2,9)	68.64
		π(2,6,1,5)$\otimes\nu$(4,6,2,9)	10.15
$21/2^-$	3064	π(4,6,1,3)$\otimes\nu$(4,6,2,9)	75.27
$25/2^-$	3776	π(4,6,1,3)$\otimes\nu$(4,6,2,9)	76.61
$27/2^-$	4396	π(4,6,1,3)$\otimes\nu$(4,6,2,9)	80.64
$29/2^-$	4975	π(4,6,1,3)$\otimes\nu$(4,6,2,9)	82.57
$31/2^-$	5258	π(4,6,1,3)$\otimes\nu$(4,6,2,9)	81.62

ACKNOWLEDGMENTS

We are grateful to the INFN-LNL staff for providing stable ^{6}Li beam throughout the experiment. This work is supported by the National Nature Science Foundation of China under Grant Nos. 11975040, U2167204 and U1832130. Z. Huang is supported by the China Scholarship Council (CSC). M. Siciliano is supported by U.S. Department of Energy, Office of Science, Office of Nuclear Physics, under the Contract No. DE-AC02-06CH11357. S. P. Hu is supported by Guangdong Key Research And Development Program 2020B040420005, Shenzhen Universities Stable Support Program 20200813080048001, and Foundation of National Laboratory of Heavy Ion Accelerator of Lanzhou 20200602SZU. C. X. Yuan is supported by the Guangdong Major Project of Basic and Applied Basic Research (2021B0301030006).

[1] A. De-Shalit, Phys. Rev. **122**, 1530 (1961).
[2] T. J. Gray, *et al.*, Phys. Rev. Lett **124**, 032502 (2020).
[3] K. Yanase and N. Shimizu, *et al.*, Phys. Rev. C **102**, 065502 (2020).
[4] M. S. M. Gerathy, *et al.*, Phys. Lett. B **823**, 136738 (2021).
[5] V. Karayonchev, *et al.*, Phys. Rev. C **103**, 044309(2021).
[6] Z. Huang *et al.*, Submitted to Phys. Rev. C.
[7] A. Nilsson and M. Grecescu, Nucl. Phys. A **212**, 448-464 (1973).
[8] H. Ohnuma and J.L. Yntema, Phys. Rev. **178**, 1855-1863 (1969).
[9] P. Singh, R. G. Pillay, J. A. Sheikh, and H. E. Devare, Phys. Rev. C **48**, 4: 1609-1616 (1993).
[10] S Ray *et al.*, Phys. Rev. C **69**, 054314 (2004).
[11] Z. Huang *et al.*, Eur. Phys. J. A **57**, 137 (2021).
[12] S. E. Arnell, *et al.*, Phys. Rev. C **49**, 1: 51-65 (1994).
[13] A. Goasduff, D. Mengoni, F. Recchia, J.J. Valiente-Dobon, et al. Nucl. Instrum. Methods. Phys. Res. A 1015, 165753 (2021).
[14] J. Gutleber, S. Murray, and L. Orsini, Computer Physics Communications **153**, 155-163 (2003).
[15] D. Barientos, *et al.*, Nuclear Science **62**, 3134 (2015).
[16] S. P. Hu *et al.*, Nucl. Instrum. Methods in Phys. Res. A **914**, 64 (2019).
[17] R. Zhen *et al.*, Phys. Rev. C **106** 024323 (2022).
[18] M. Piiparinen *et al.*, Nuclear Physics A **605**, 191 (1996).
[19] J.-M Régis *et al.*, Nucl. Instrum. Methods Phys. Res. A **606**, 466 (2009).
[20] N. Shimizu *et al.*, Comp. Phys. Comm. **244**, 372 (2019).
[21] M. Honma *et al.*, Phys. Rev. C **80**, 064323 (2009).
[22] N.S. Pattabiraman, *et al.*, Phys. Rev. C. **65**, 044324 (2002).
[23] S. Cochavi, *et al.*, Phys. Rev. C **3**, 1352 (1971).
[24] https://www-stone.ch.cam.ac.uk/wigner.shtml.